

## SHAPE SLOPE PARAMETER DISTRIBUTION MODELLING OF ELECTROMAGNETIC SCATTERING BY RAIN DROPS

**L. S. Kumar and Y. H. Lee**

Nanyang Technological University  
50, Nanyang Avenue, Singapore

**J. T. Ong**

Research and Technology  
C2N Pte. Ltd.  
41, Cheng Soon Garden, Singapore

**Abstract**—Gamma model parameters using 2nd, 3rd and 4th moments are calculated from the drop size data of Singapore. The gamma model is simplified into two parameter model by finding a relation between the shape and slope parameters,  $\mu$  and  $\Lambda$ . Due to the poor correlation found between  $\mu$  and  $\Lambda$ , the drop size data is filtered based on their rain rates before a good correlation between the two parameters can be found. The  $\mu$ - $\Lambda$  relations are then fitted for the different ranges of rain rate filtering. Scatter plots of  $\mu$  and  $\Lambda$  are plotted with constant median volume diameter ( $D_0$ ) lines. The  $\mu$ - $\Lambda$  relations for the different rain types for the tropical island of Singapore are proposed and compared with the  $\mu$ - $\Lambda$  relations from three other countries of different climatic zones. T-Matrix calculations are performed to find the polarimetric variables at S-band by using the gamma DSD calculated from the Singapore's drop size data. The calculated differential reflectivity and horizontal reflectivity are used along with the best  $\mu$ - $\Lambda$  relations to find the gamma model parameters. The retrieved rain rate using polarimetric variables is compared with the distrometer's measured rain rate. Results show a good agreement between the retrieved rain rate and the measured rain rate. Therefore, the proposed shape slope relationship is found to be suitable for rain rate retrieval.

## 1. INTRODUCTION

Rain rate estimation from RADAR measurements is based on empirical models such as the reflectivity and rain rate, the Z-R relation, which have been studied for more than 60 years. This empirical relation cannot give an accurate result for the rain rate estimation of different types of rain and drop size distribution (DSD). Communication systems operating at frequencies above 10 GHz in equatorial climates are subjected to many fade occurrences due to heavy rainfall [1]. Therefore, accurate estimation of rain rate is very important in order to design communication links. The use of dual polarized RADAR which has two remote measurements increases the accuracy of the rain rate estimation. Rain DSD parameters can be retrieved from two remote measurements and rain rate can be retrieved from these DSD parameters [2].

Accurate rain rate estimation requires detailed knowledge of the rain drop size distribution (DSD). The measured DSD data is fitted to a distribution in order to find the DSD parameters. Ulbrich [3] has shown that the DSD is best modeled by a gamma distribution and suggested the following form:

$$N(D) = N_0 D^\mu \exp(-\Lambda D) \quad (1)$$

where  $N(D)$  is the distribution of rain drops per diameter interval  $D$  to  $D + \Delta D$  (mm) per unit volume,  $N_0$  is the intercept parameter ( $\text{mm}^{-1-\mu} \text{m}^{-3}$ ),  $\Lambda$  is the slope of the exponential ( $\text{mm}^{-1}$ ) and  $\mu$  is the dimensionless shape parameter.

The gamma model has three parameters. In order to retrieve the three DSD parameters, three remote measurements are required from RADAR. But polarimetric RADAR has only two remote measurements, reflectivity ( $Z$ ) and differential reflectivity ( $Z_{DR}$ ). Therefore, for the purpose of retrieving the DSD parameters from remote sensing measurements, it is necessary to reduce the number of parameters of the gamma distribution to two instead of three. One of the ways to reduce the three-parameter gamma DSD to a two-parameter function is to find a relation between two of the gamma parameters. In this paper, the correlation between two of the gamma model parameters are examined in order to find a relationship between them. Two independent remote measurements and the derived empirical constraining relationship between the DSD parameters can then be used to retrieve rain rate.

It is explained in [4] that the parameterization of model distributions is well known mathematical procedure and does not have strong limitation on the number of parameters. Gurvich used a simplified model with two parameters with some assumptions instead

of finding four parameters. Similarly, in this paper, two of the other gamma model parameters are found from the remote measurements and the derived empirical constraining relationship is used to find one of the gamma model parameter.

Two dimensional video distrometer (2DVD) measurements made in Florida shows a high correlation between  $\mu$  and  $\Lambda$  [2] indicating that these parameters are related. Making use of these measurements, Zhang et al. [2] derived a second order polynomial constraining relation between  $\mu$  and  $\Lambda$  for rain rates greater than 5 mm/hr. Later, Brandes et al. [5] modified the  $\mu$ - $\Lambda$  relation to accommodate heavy rainfalls using the same data from Florida. They filtered the database to exclude rain rates smaller than 5 mm/hr, and drop counts smaller than 1000 prior to curve fitting. Zhang et al. [6] have used the  $\mu$ - $\Lambda$  relation proposed by [5] and shown that the relation contains useful information and characterizes the natural rain DSD variations well. He noted that the coefficients of the  $\mu$ - $\Lambda$  relation might change with location and season. He has also shown that the  $\mu$ - $\Lambda$  relation might be valid for convective precipitation but may fail in weak, stratiform rain. Both Zhang et al. [2] and Brandes et al. [5] used 2nd, 4th and 6th moments to fit the gamma model.

Seifert [7] examined the validity of  $\mu$ - $\Lambda$  relation and concluded that this relation is the fundamental property of rain DSD. He found a good agreement between the empirical  $\mu$ - $\Lambda$  relations that he has derived with that by Zhang et al. [2]. This is especially true for the convective and stratiform DSDs except at leading edges of convective storms and drizzle rains. He also found that for strong rain events,  $\mu$  is much larger in increasing rain than in decreasing rain, resulting in the data points lying above the empirical  $\mu$ - $\Lambda$  relation derived by [2]. The weakest precipitation events having rain rates less than 10 mm/hr shows lower  $\mu$  values below the empirical  $\mu$ - $\Lambda$  relation derived by [2].

Moisseev and Chandrasekar [8] attributed the  $\mu$ - $\Lambda$  relation to the effect of moment errors. They explained that the correlation between the shape and slope parameters was mainly due to the truncation of small raindrops ( $\leq 0.6$  mm) and data filtering. But the  $\mu$ - $\Lambda$  relation has been successfully applied for rain retrievals using polarimetric RADAR measurements of reflectivity ( $Z_H$ ) and differential reflectivity ( $Z_{DR}$ ) [5, 9, 10]. Cao and Zhang [11] found that the  $\mu$ - $\Lambda$  relation is practically equivalent to the mean function of normalized DSDs proposed by Testud. Testud's relation is free of any assumed DSD form and is not affected by the errors of functional fitting. He concluded that the equivalence between the  $\mu$ - $\Lambda$  relation and Testud's function indicates the physical information in the  $\mu$ - $\Lambda$  relation of the constrained-gamma (C-G) model proposed by [2].

Narayana et al. [12] studied the variability of the  $\mu$ - $\Lambda$  relation using the Joss-Waldvogel distrometer (JWD) data measured at Gadanki, India, under the conditions, reflectivity  $\geq 30$  dBZ and number of drops  $\geq 500$ . They used 3rd, 4th and 6th moments to fit the gamma model. Recently, Brawn and Upton [13] fitted the  $\mu$ - $\Lambda$  relation for rain rates greater than 1 mm/hr based on their drop size data measured at Dumfries and Galloway, Scotland, using the Thies and Parsivel distrometers. The procedure described by Brawn and Upton [13] to estimate the values of gamma parameters was used. They filtered all the rain rates less than 1 mm/hr from their drop size data to fit the relation. It was concluded that the relation appears to vary with the type of distrometer used. Munchak and Tokay [14] fitted the  $\mu$ - $\Lambda$  relation for different reflectivity ranges for nine different regions and concluded that the  $\mu$ - $\Lambda$  relations perform best at high reflectivity ( $> 35$  dBZ). In general, the use of  $\mu$ - $\Lambda$  relation is proven to perform well for DSD retrieval [5, 9, 10]. Atlas and Ulbrich [15] explained that the  $\mu$ - $\Lambda$  correlations proposed by [2, 5] appear to be limited to rainfall events which do not include convective rain; they are biased toward stratiform and transition rains. Therefore, in this paper, a rain event is classified according to the rain rate and median volume diameter variations before deriving the  $\mu$ - $\Lambda$  relations.

Tokay and Short [16] have found using the distrometer and wind profiler measurements that values of  $R < 2$  mm/hr are representative of stratiform spectra (which lead to significant rain accumulation) while values of  $R > 10$  mm/hr are representative of convective ones (relatively short in duration and highly fluctuating). Caracciolo [17] used the Pludix exponential DSD parameters for all Italian databases and found that the precipitation types are changing from stratiform (with  $R < 2$  mm/hr) to convective (with  $R > 10$  mm/hr). Therefore, three different categories of rain rates,  $R < 2$  mm/hr (stratiform),  $2 \text{ mm/hr} \leq R < 10 \text{ mm/hr}$  (stratiform, transition and convective type rain) and  $R \geq 10 \text{ mm/hr}$  (convective type rain), are considered in order to fit the  $\mu$ - $\Lambda$  relations for the 996 minutes of drop size data for Singapore. The rain categorization used by [5, 12, 13] are also considered for the  $\mu$ - $\Lambda$  relations fitting purposes, so as to provide a fair comparison of the different types of rains at the different climatic zones.

T-Matrix calculations are performed for the 1-minute integrated DSDs for the entire data set. Polarimetric RADAR variables from the T-Matrix calculations and best  $\mu$ - $\Lambda$  relations are used to find gamma DSD parameters. The rain rate retrieved using the calculated gamma DSD is compared with the measured rain rate.

## 2. DATA SELECTION AND MEASUREMENT

Data recorded from August 1994 to September 1995; (excluding June and July 1995) using a Joss-Waldvogel distrometer RD-69 is used in this study. The dead-time correction has been applied using the software provided by Distromet, Inc. The correction is intended to correct up to 10% of the accuracy. Only DSDs having a number of rain drops greater than 10 are considered, resulting in a total of 996 minutes of data from 14 rain events.

Most rain events in Singapore reach maximum intensity very rapidly; the rain event remains heavy for a few minutes, and then decreases slowly before increasing again. Lower rain rates usually occur during the decreasing period. One rain event is defined from the beginning till the end of the rainfall. The events chosen for this analysis have peak rain rates from 28.04 mm/hr to 191.59 mm/hr.

The rain rate (in mm/hr) and reflectivity (in  $\text{mm}^{-6}\text{m}^3$ ) can be calculated from the measured data by

$$R = \frac{3600\pi}{6ST} \sum_{i=1}^{20} D_i^3 n_i \quad (2)$$

$$z = \frac{10^6}{ST} \sum_{i=1}^{20} \frac{D_i^6 n_i}{v(D_i)} \quad (3)$$

where  $n_i$  is the number of rain drops in the  $i$ th channel,  $D_i$  is the mean drop diameter in mm,  $S = 5000 \text{ mm}^2$  is the sample area,  $T = 60 \text{ sec}$  is the integration time and  $v(D_i)$  is the terminal velocity of rain drop in m/s obtained from Gunn and Kinzer [18].

In order to fit the drop size distribution, gamma model is used. The moment estimators frequently used to estimate parameters for drop size distribution (DSD) functions are biased [19]. This bias tends to be stronger when higher-order moments are used. The low-order moments for observed drop size data involve substantial uncertainties because of deficiencies in the observations of the smallest raindrops [19]. The middle moments generally have lower measurement errors. The 2nd, 3rd and 4th moments have a relatively better estimation of integral RADAR/rain parameters than other moments if DSD follows the gamma distribution [11]. Therefore, in this paper, the central moments, 2nd, 3rd and 4th are used to fit gamma model.

### 3. RESULTS AND DISCUSSIONS

#### 3.1. Rain Classification

Figure 1 shows a rain event in Singapore on the November 12th, 1994. The rain event is classified into three different rain types, convective, stratiform and transition, by using the method proposed in [20]. The classification is done by using both the rain rate,  $R$ , and the median volume diameter,  $D_0$ , variations. The plot shows the rain rate and median volume diameter variations for 240 minutes of duration during this rain event.  $R = 2$  mm/hr and  $R = 10$  mm/hr lines are drawn to indicate the boundaries between the convective and stratiform stages. As shown, most of the convective points lie above 10 mm/hr, whereas the stratiform points are below 2 mm/hr. The transition points are either between the two rain rates or above the rain rate of 10 mm/hr.

The rain event has two convective peaks followed by transition and stratiform stages. The first convective peak, known as stage C1, from 0 to 52 minutes, is characterized by DSDs of large  $D_0$  and large  $R$ . The second convective stage, C2, from 53 to 128 minutes, has slightly smaller  $D_0$  and maximum  $R$ . The stage following C2 is the transition stage, T, which can clearly be distinguished from stages C1 and C2 by the reduction in  $D_0$ , less than 1.5 mm, and also the rapid reduction in rain rate. After 129 minutes of convective rain, both  $R$  and  $D_0$  decrease continuously and reach a minimum with  $D_0 = 0.93$  mm and

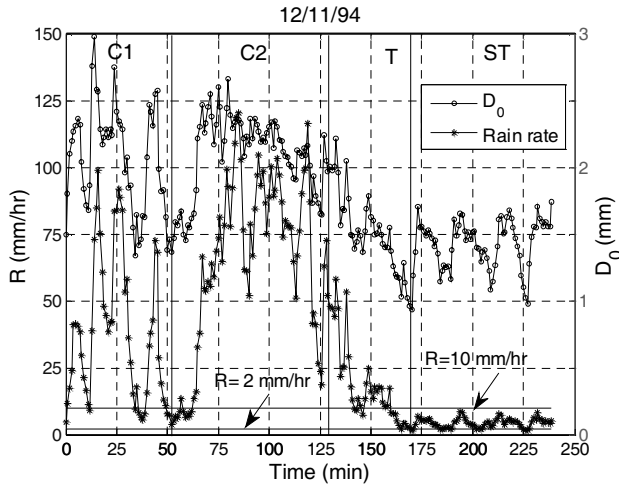


**Figure 1.** Classification of Joss-Waldvogel distrometer data, recorded on November 12th, 1994.

$R = 1.53$  mm/hr at 170 minutes. After that, both parameters start to increase again, indicating the beginning of the stratiform stage, ST. In the steady stratiform stage with duration of 69 minutes,  $D_0$  fluctuates around 1.5 mm and  $R$  is always less than 10 mm/hr. It is clear from Fig. 1 that the rain rates above 10 mm/hr mainly consist of convective type rain and rain rates less than 2 mm/hr only consist of stratiform points. The intermediate rain category  $2 \text{ mm/hr} \leq R < 10 \text{ mm/hr}$  exhibits all the three rain types.

### 3.2. $\mu$ - $\Lambda$ Relationship

Three of the 14 rain events over 996 minutes of DSD have a similar rain structure. Five rain events have only one convective stage followed by a stratiform stage. Six events have either one convective stage or two convective stages without a stratiform stage. All 14 events, including the one explained above, are filtered based on the rain rates before fitting the  $\mu$ - $\Lambda$  relations. Gamma model parameters are calculated for the 14 major rain events. DSD minutes are filtered using the rain categories,  $R < 2$  mm/hr,  $2 \text{ mm/hr} \leq R < 10$  mm/hr and  $R \geq 10$  mm/hr. The subplots of Fig. 2 show the scatter plot of  $\mu$  and  $\Lambda$  for the three rain categories respectively. Solid lines with markers are the proposed  $\mu$ - $\Lambda$  relations fittings. A linear fit for the rain category,  $R < 2$  mm/hr, and polynomial fits for the other two rain categories are suggested.

In order to show the size of  $D_0$ , the median volume diameter, within the three rain categories, the scatter plots are plotted using different symbol shapes corresponding to the different range of  $D_0$  as shown in the legend in subplot 2 of Fig. 2. The lines of constant  $D_0$  were derived based on the relationship  $D_0 = (3.67 + \mu)/\Lambda$  in [15] for a gamma DSD and are drawn in the figure for  $D_0 = 4, 3, 2$  and 1. These constant  $D_0$  lines show the variation in size of  $D_0$  for the different rain categories.

It is clear from Fig. 2 that the variation between the  $\mu$  and  $\Lambda$  values is large, and there is a low correlation between the two parameters at low rain rates. However, the correlation increases for the lower  $\mu$  and  $\Lambda$  values, especially for the rain category with high rain rates,  $R \geq 10$  mm/hr. This increase in correlation is due in large to the reduction of errors in the parameter estimates that occurs with increasing number of sample size at higher rainfall rates. The spread of scattered  $\mu$  and  $\Lambda$  points in Fig. 2, are also due to measurement errors, which are relatively larger for low rain rates than high rain rates [6]. Tokay et al. [21] compared the video distrometer and Joss distrometer drop size measurements. He concluded that the JWD has a larger measurement error because of the insufficient measurement of small

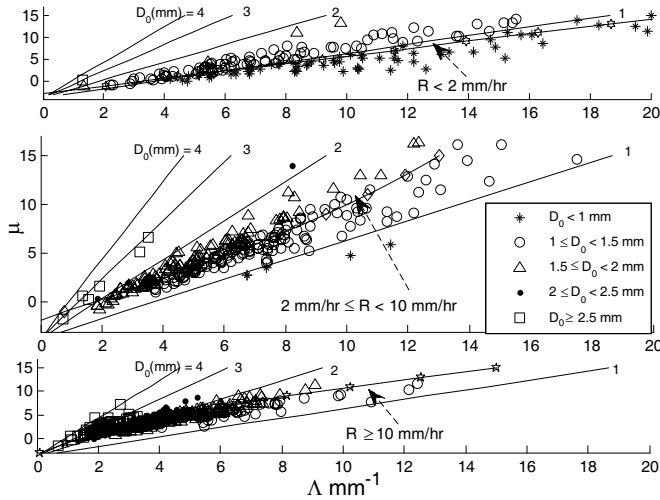


**Figure 2.** Scatter plots of  $\mu$ - $\Lambda$  values obtained for the rain categories,  $R < 2$  mm/hr (subplot 1),  $2$  mm/hr  $\leq R < 10$  mm/hr (subplot 2) and  $R \geq 10$  mm/hr (subplot 3) from Singapore's DSD for a total of 996 DSD minutes. The rain categories, for which scatters and  $\mu$ - $\Lambda$  relations are displayed, are written as text in the subplots. The solid lines with markers are their corresponding fitted  $\mu$ - $\Lambda$  relations respectively. The different symbols used correspond to ranges of median volume diameter,  $D_0$ , in the subplots as in the legend in subplot 2. The straight lines labeled with values of constant  $D_0$  correspond to the theoretical relation  $D_0 = (3.67 + \mu)/\Lambda$ .

raindrops at rain rates above 20 mm/hr, also called dead time effect. He also found that the JWD severely underestimated only at very small drop sizes (diameter  $< 0.5$  mm). Since JWD is the measuring instrument used in this study, the larger measurement error leads to the poor correlation between  $\mu$  and  $\Lambda$  values.

As can be seen from Fig. 2, the spread of the scatters, for  $R < 2$  mm/hr, is large with most of them having diameter sizes of  $D_0$  less than 1 mm to 2 mm. One of these scatters has  $D_0$  of around 3 mm. For  $2$  mm/hr  $\leq R < 10$  mm/hr, the scatters fall between  $D_0$  of 1–2 mm. Therefore most of the scatters have either triangular or circle shapes. The scatters for  $R \geq 10$  mm/hr show a good correlation between the  $\mu$  and  $\Lambda$  values with most of them having diameter sizes from  $D_0$  around 1.5 mm to greater than 3 mm. It is evident from subplot 3 of Fig. 2 that the shapes of the scatters are triangle,  $D_0 = 1.5$  mm to 2 mm, point,  $D_0 = 2$  mm to 2.5 mm or square,  $D_0 \geq 2.5$  mm. There are no drops



with sizes less than 1 mm and only few drops between 1 mm to 1.5 mm. This indicates that drop sizes increase as the rain rate increases. The  $\mu$ - $\Lambda$  relation derived for the rain category,  $R \geq 10$  mm/hr consists of only convective rain and has higher  $\mu$  values, whereas  $R < 2$  mm/hr consist of stratiform rain and has lower  $\mu$  values. The  $\mu$ - $\Lambda$  fit for the rain category  $2 \text{ mm/hr} \leq R < 10 \text{ mm/hr}$  is in between the two fits ( $R < 2 \text{ mm/hr}$  and  $R \geq 10 \text{ mm/hr}$ ) since it contains all three rain types.

Table 1 shows the rain categories, the coefficients of the  $\mu$ - $\Lambda$  relations with 95% confidence bounds and Pearson correlation coefficients. The different rain categorizations, i.e.,  $R \geq 5$  mm/hr & drops  $\geq 1000$  used by Brandes et al. [5],  $z \geq 30$  dBZ & drops  $\geq 500$  used by Narayana et al. [12], and  $R \geq 1$  mm/hr used by Brawn and Upton [13], are also included in the table for comparison with other published results. As can be seen in Table 1, for the rain categories for which there are more lower rain rates included, such as  $R < 2$  mm/hr and  $R \geq 1$  mm/hr, the coefficient ‘C’ of the polynomial fit is not only negative, but very small, with values of  $-0.004$  and  $-0.005$  respectively. Therefore, a linear fit is proposed for these categories. The resultant coefficients from the linear fit are included in the last rows of Table 1. The rain category  $R \geq 1$  mm/hr which have almost all the three rain types has the lower Pearson coefficient of 0.89. It is clear from Pearson coefficients of filtered rain categories that filtering increases

**Table 1.** The coefficients of the  $\mu$ - $\Lambda$  relations with 95% confidence bounds and Pearson correlation coefficients for different category of rain rates.

| Splitting criteria                   | $\Lambda = C\mu^2 + B\mu + A$ |                       |                      | Pearson Correlation Coefficient |
|--------------------------------------|-------------------------------|-----------------------|----------------------|---------------------------------|
|                                      | C                             | B                     | A                    |                                 |
| $R < 2$ mm/hr                        | -0.0043 (-0.0063, -0.0024)    | 1.437 (1.311, 1.563)  | 1.948 (0.875, 3.02)  | 0.93                            |
| $2 \text{ mm/hr} \leq R < 10$ mm/hr  | -0.0148 (-0.0190, -0.0105)    | 0.970 (0.886, 1.055)  | 1.776 (1.447, 2.104) | 0.92                            |
| $R \geq 10$ mm/hr                    | 0.026 (0.0161, 0.036)         | 0.516 (0.422, 0.610)  | 1.424 (1.225, 1.623) | 0.90                            |
| $R \geq 5$ mm/hr & drops $\geq 1000$ | 0.051 (0.0351, 0.0672)        | 0.351 (0.198, 0.503)  | 1.696 (1.371, 2.02)  | 0.87                            |
| $z \geq 30$ dBZ & drops $\geq 500$   | 0.030 (0.01882, 0.04216)      | 0.558 (0.451, 0.6662) | 1.418 (1.19, 1.645)  | 0.89                            |
| $R \geq 1$ mm/hr                     | -0.005 (-0.0091, -0.0015)     | 0.938 (0.87, 1.005)   | 1.034 (0.808, 1.26)  | 0.89                            |
| * $R < 2$ mm/hr                      | X                             | 1.188 (1.123, 1.252)  | 3.247 (2.297, 4.197) | 0.93                            |
| * $R \geq 1$ mm/hr                   | X                             | 0.852 (0.823, 0.882)  | 1.254 (1.091, 1.416) | 0.89                            |

\* – Represents linear fits

the correlation between the shape and slope parameters except for the filtering  $R \geq 5$  mm/hr & drops  $\geq 1000$ . This rain category has mostly convective points but has some stratiform points and these results in the slight decrease of Pearson coefficient.

Rain rate in mm/hr and reflectivity in  $\text{mm}^{-6}\text{m}^3$  are then calculated for gamma models using the  $\mu$ - $\Lambda$  relationships for all the above categories using,

$$R = 6\pi \times 10^{-4} \sum_{i=1}^{20} D_i^3 v(D_i) N(D_i) \Delta D_i \quad (4)$$

$$z = \sum_{i=1}^{20} D_i^6 N(D_i) \Delta D_i \quad (5)$$

For gamma models using  $\mu$ - $\Lambda$  relationships,  $\mu$  is calculated from the fitted gamma DSD,  $\Lambda$  is calculated using the  $\mu$ - $\Lambda$  relation for the corresponding rain category and  $N_0$  is fitted using these  $\mu$  and  $\Lambda$  values. To evaluate the accuracy of the  $\mu$ - $\Lambda$  relationships, the root mean square deviation in rain rate estimation ( $RMSD$ - $R$  in dB) and the root mean square deviation in reflectivity estimation ( $RMSD$ - $z$  in dB) are used. They are calculated by,

$$RMSD-R = 10 \times \sqrt{\frac{1}{c} \sum_{i=1}^c (\log_{10} R_{cali} - \log_{10} R_{meai})^2} \quad (6)$$

$$RMSD-z = 10 \times \sqrt{\frac{1}{c} \sum_{i=1}^c (\log_{10} z_{cali} - \log_{10} z_{meai})^2} \quad (7)$$

where  $c = 996$  is the number of data points.  $R_{meai}$  and  $z_{meai}$  are calculated from the measured data using (2) and (3) respectively.  $R_{cali}$  and  $z_{cali}$  are the calculated rain rate and reflectivity from (4) and (5) from the gamma modeled DSD using  $\mu$ - $\Lambda$  relations. Since the gamma models using  $\mu$ - $\Lambda$  relationships are fitted using the 2nd, 3rd and 4th moments fitting procedure, the root mean square errors contain two parts, one is due to the 2nd, 3rd and 4th moments fitting procedure and the other error is the model error of  $\mu$ - $\Lambda$  relation. But the error due to the 2nd, 3rd and 4th moments fitting procedure is common for all the rain categories. Therefore the differences in errors are considered as the differences in the model errors of  $\mu$ - $\Lambda$  relations.

Table 2 shows the rain categories and the  $RMSD$ - $R$  and  $RMSD$ - $z$  of the gamma models using the corresponding  $\mu$ - $\Lambda$  relations.

Smaller errors are produced in both rain rate and reflectivity estimation for the higher rain categories,  $R \geq 10$  mm/hr,  $R \geq 5$  mm/hr

**Table 2.** *RMSD-R* and *RMSD-z* values with measured data for different category of rain rates.

| Splitting criteria                           | <i>RMSD-R</i> | <i>RMSD-z</i> |
|--|---------------|---------------|
| $R < 2 \text{ mm/hr}$                        | 2.50          | 5.38          |
| $2 \text{ mm/hr} \leq R < 10 \text{ mm/hr}$  | 1.27          | 2.82          |
| $R \geq 10 \text{ mm/hr}$                    | 1.13          | 2.89          |
| $R \geq 5 \text{ mm/hr}$ & drops $\geq 1000$ | 1.15          | 2.91          |
| $z \geq 30 \text{ dBZ}$ & drops $\geq 500$   | 1.25          | 3.10          |
| $R \geq 1 \text{ mm/hr}$                     | 1.87          | 4.46          |
| * $R < 2 \text{ mm/hr}$                      | 2.28          | 4.86          |
| * $R \geq 1 \text{ mm/hr}$                   | 1.85          | 4.39          |

\* — Represents linear fits

& drops  $\geq 1000$ ,  $z \geq 30 \text{ dBZ}$  & drops  $\geq 500$  and  $2 \text{ mm/hr} \leq R < 10 \text{ mm/hr}$ . This is because, there is a reduction in the variability of the gamma model parameters and thus a reduction in errors at higher rain rates as the sample size increases at higher rain rates. The deficiency in the measurement of small rain drops by JWD, measuring instrument, is also the reason for the higher errors at the lower rain rates. The lowest rain categories,  $R < 2 \text{ mm/hr}$ ,  $R \geq 1 \text{ mm/hr}$  have higher RMSD compared to the other higher rain rate categories.

As can be seen from Table 2, *RMSD-R* is always less than the *RMSD-z*. This is because, the calculation of the gamma model parameters uses the 2nd, 3rd and 4th moments. Those moments are closer to the value of  $R$ , which is related to 3.67th moment. Thus, one would expect relatively small values of *RMSD-R*, regardless of the  $\mu$ - $\Lambda$  relations. Therefore, the *RMSD-z*, for the estimation of reflectivity,  $z$ , related to 6th moment, a quantity far from the 2nd, 3rd and 4th moments, is also included in this paper to examine how well the  $\mu$ - $\Lambda$  relations match with the measured data. Even though the errors in reflectivity estimation are higher compared to the errors in rain rate estimation, the trend is same. The rain categories with the higher rain rates produce smaller errors compared to the rain categories with lower rain rates. For the rain categories,  $R < 2 \text{ mm/hr}$  and  $R \geq 1 \text{ mm/hr}$ , by comparing the polynomial and linear fits, the linear fit is found to be better, since the error in rain rate and reflectivity estimation is small. The linear fit is less complex than the polynomial fit, and therefore, the linear fit is recommended.

Figure 3 shows the  $\mu$ - $\Lambda$  fits of Singapore with different filtering; the three proposed rain categories;  $R \geq 5 \text{ mm/hr}$  & drops  $\geq 1000$ ;

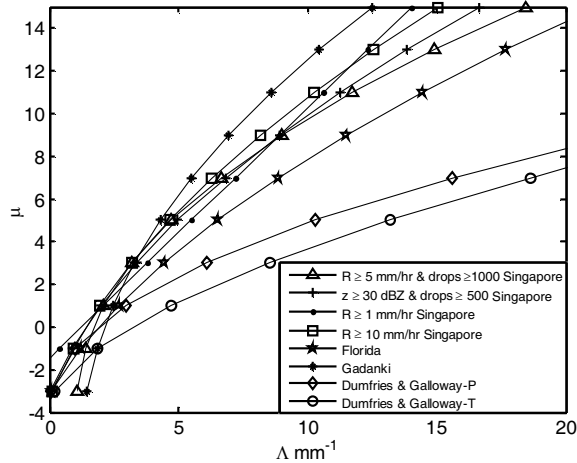


**Figure 3.** The  $\mu$ - $\Lambda$  relations of Florida, Gadanki, and Dumfries and Galloway along with the  $\mu$ - $\Lambda$  relations of Singapore for different filtering criteria.

$z \geq 30$  dBZ & drops  $\geq 500$ ; and  $R \geq 1$  mm/hr. The  $\mu$ - $\Lambda$  fits for the following are also plotted for comparison with the Singapore data: Florida with the filtering,  $R \geq 5$  mm/hr & drops  $\geq 1000$  [5]; Gadanki with filtering  $z \geq 30$  dBZ & drops  $\geq 500$  [12]; and Dumfries & Galloway (DG), with filtering  $R \geq 1$  mm/hr [13].

For the data from Scotland, two sets of  $\mu$ - $\Lambda$  fits are provided: The Dumfries & Galloway-P for the Parsivel distrometer; and the Dumfries & Galloway-T for the Thies distrometer. In Fig. 3, the Singapore fit for the rain category  $R \geq 10$  mm/hr is included to show that the results with this filtering for the Singapore data are closer to those from Gadanki. As seen from Fig. 3, all the Singapore fits for the rain categories,  $R \geq 10$  mm/h,  $R \geq 5$  mm/hr & drops  $\geq 1000$ ,  $z \geq 30$  dBZ & drops  $\geq 500$  and  $R \geq 1$  mm/hr, lie between the Gadanki and Florida fits. Even though different filtering criteria are used, the fits of Singapore do not differ much.

The Gadanki curve has higher  $\mu$  values than the Singapore fits, which indicates that their data consists mainly of convective rain events. The  $\mu$ - $\Lambda$  relation derived from Singapore's data for the rain category,  $R \geq 10$  mm/hr consists of only convective type rain and therefore follows Gadanki, especially for  $\mu$  values greater than 2. The use of JWD in the two above locations is also a reason for the closeness of Gadanki and Singapore fits. As explained in Section 3.2, the deficiency of the JWD to measure smaller drops also results the

Singapore and Gadanki curves with higher  $\mu$  values. Singapore curves used 2nd, 3rd and 4th moments whereas Gadanki curve uses 3rd, 4th and 6th moments to fit the gamma model. The use of the higher moments to fit the gamma model leads to the higher  $\mu$  values of Gadanki fit.

Also seen from Fig. 3,  $\mu$  values of the Florida curve are lower than the Gadanki and Singapore fits but higher than DG fits. The trend of the  $\mu$ - $\Lambda$  fit of Singapore for the filtering,  $R \geq 5$  mm/hr & drops  $\geq 1000$  follows the Florida curve for  $\mu > 4$ . This indicates that the rain events used in [5] are near to the stratiform and transition type rains. This may be the reason, as explained by Seifert [7], for the lower  $\mu$  values of Florida as compared to Singapore's  $\mu$  values at lower rain rates. In Fig. 3, the two fits from DG have very low  $\mu$  values compared to all other fits, indicating very weak events in Scotland. This agrees with Zhang's statement [6] that  $\mu$ - $\Lambda$  relations vary with the location since each location has different types of rain. Another reason for their fit to have a low  $\mu$  value is the use of different distrometers and their use of a new procedure to estimate the gamma parameters. Their two fits, although different in value, have the same trend. The difference in value is due to the different measurement devices. Florida uses the video distrometer, DG uses two different laser distrometers, whereas Gadanki and Singapore use the JWD.

It is concluded from the above fits that the type of rain events, climatic zones, the fitting procedures to model DSD and the type of measuring devices will cause the  $\mu$ - $\Lambda$  relations to differ. The  $\mu$ - $\Lambda$  fits for the categories,  $R \geq 10$  mm/hr,  $R \geq 5$  mm/hr & drops  $\geq 1000$ ,  $5$  mm/hr  $\leq R < 10$  mm/hr and  $z \geq 30$  dBZ & drops  $\geq 500$ , produce smaller errors as compared to the  $\mu$ - $\Lambda$  fits of lower rain rate categories. The use of JWD leads to measurement errors especially in the measurement of smaller rain drops is also the reason for the increase of root mean square deviation at lower rain rates.

Two of the best fits for the rain categories,  $R \geq 10$  mm/hr and  $R \geq 5$  mm/hr & drops  $\geq 1000$ , which produce minimum errors in rain rate and reflectivity estimation are used to calculate the rain rate from the polarimetric RADAR variables. These variables are calculated using the T-Matrix code and can be used for retrieving the rain rate.

### 3.3. Rain Rate Retrieval

Thurai et al. [22] performed the T-Matrix calculations for 1-minute integrated DSDs. They fitted the DSDs using the normalized gamma distributions. Calculations were made at C band to derive  $Z_{hh}$ ,  $Z_{dr}$  and attenuation values for over 1600 one-minute DSDs measured during a subtropical rain event. The water temperature was set to 20°C

and a canting angle distribution with zero mean and  $5^\circ$  standard deviation was used in their calculations. They compared the T-Matrix calculations based on the contoured shapes and their oblate approximations proposed by them.

In this paper, T-Matrix calculations are performed as similar at S band, 2.72 GHz for the Beard and Chung drop shape model [23]. The calculations are done at the elevation angle of  $1^\circ$  for the water temperature of  $20^\circ\text{C}$ . The canting angle distribution with zero mean and  $10^\circ$  standard deviation is used for Singapore's tropical climate. Gamma DSD using 2nd, 3rd and 4th moments, calculated from the Singapore's drop size data is used as an input to the T-Matrix code. The calculated polarimetric RADAR variables, differential reflectivity ( $Z_{dr}$ ) in dB and horizontal reflectivity ( $Z_{hh}$ ) in  $\text{mm}^{-6}\text{m}^3$  are then used to find the gamma model parameters. Fig. 4 shows the relation  $Z_{dr}$  versus  $\Lambda$  and  $Z_{hh}/N_0$  versus  $\Lambda$  where the values  $N_0$  and  $\Lambda$  are from the gamma DSD fitted using 2nd, 3rd and 4th moments.

The procedure explained in [2] is used to find gamma model parameters from  $Z_{dr}$  and  $Z_{hh}$ . Using Fig. 4,  $\Lambda$  can be inferred for a specified  $Z_{dr}$  and then using the inferred  $\Lambda$  and  $Z_{hh}$ , the parameter  $N_0$  can be obtained. Shape parameter,  $\mu$  is calculated using the best  $\mu$ - $\Lambda$  relations for the rain categories  $R \geq 10$  mm/hr and  $R \geq 5$  mm/hr & drops  $\geq 1000$ . The rain event on February 26th, 1995 is used as an example for the retrieval of polarimetric RADAR variables. Fig. 5 shows the measured rain rate and retrieved rain rates from the polarimetric RADAR variables using the best  $\mu$ - $\Lambda$  relations derived in Section 3.2 for 14 rain events, 996 minutes of drop size data, including the rain event on the February 26th, 1995.

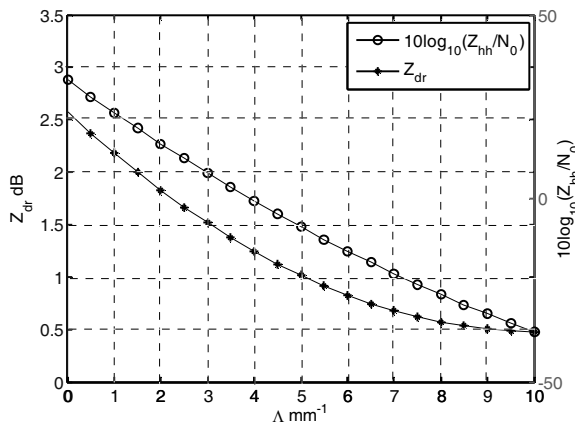


**Figure 4.** Dependence of  $Z_{dr}$  and  $10 \log_{10}(Z_{hh}/N_0)$  on  $\Lambda$ .

The rain event in Fig. 5 has two convective peaks with a maximum rain rate of 162 mm/hr and lasts for around three hours. The duration of rain event is from 1025 minutes to 1170 minutes. Good agreement can be seen between the distrometer measurement and the  $\mu$ - $\Lambda$  relation retrievals from polarimetric RADAR variable measurements. As can be seen from Fig. 5, for lower rain rates less than 80 mm/hr, rain retrieval using the  $\mu$ - $\Lambda$  relation for  $R \geq 5$  mm/hr & drops  $\geq 1000$  is better than the rain retrieval using the  $\mu$ - $\Lambda$  relation for  $R \geq 10$  mm/hr.

The rain retrieval using the  $\mu$ - $\Lambda$  relation for  $R \geq 10$  mm/hr slightly overestimates the measured rain rate at lower rain rates; this is because the  $\mu$ - $\Lambda$  relation for  $R \geq 10$  mm/hr has only convective points. As can be seen from Fig. 3, the  $\mu$  values of the rain categories  $R \geq 1$  mm/hr,  $z \geq 30$  dBZ & drops  $\geq 500$ ,  $R \geq 5$  mm/hr & drops  $\geq 1000$  and  $R \geq 10$  mm/hr increase in ascending order. Therefore the  $\mu$ - $\Lambda$  relation for the rain category,  $R \geq 10$  mm/hr which has higher  $\mu$  values compared to all the other fits slightly overestimates at the lower rain rates. But it is clear from Fig. 4 that the rain rates using the  $\mu$ - $\Lambda$  relation for  $R \geq 10$  mm/hr are closer to the measured rain rates than the rain rates calculated using the  $\mu$ - $\Lambda$  relation for  $R \geq 5$  mm/hr & drops  $\geq 1000$  at higher rain rates especially near the convective peaks. Therefore, the  $\mu$ - $\Lambda$  relation for  $R \geq 5$  mm/hr & drops  $\geq 1000$  can be used for the retrieval at all the rain rates whereas the  $\mu$ - $\Lambda$  relation for  $R \geq 10$  mm/hr can be used for accurate rain estimation for convective rain events.

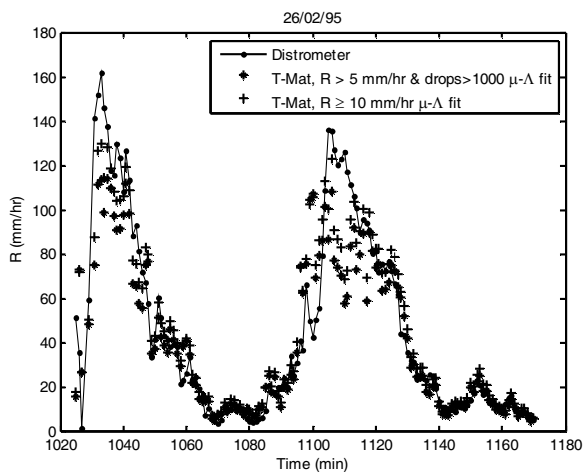


**Figure 5.** Comparison of rain rates retrieved using the  $\mu$ - $\Lambda$  relations with measured rain rate for the rain event on 26/02/1995.

#### 4. CONCLUSION

The gamma model is fitted using 2nd, 3rd and 4th moments to represent the rain drop size distribution of Singapore. The three parameter gamma model can be simplified into two parameter gamma model which can be retrieved from two remote measurements to find rain rate. Therefore, the correlation between the gamma model parameters,  $\mu$  and  $\Lambda$  are checked in order to find the relation between them. It is found that filtering the rain rates improve the correlation between  $\mu$  and  $\Lambda$ . Therefore, the  $\mu$ - $\Lambda$  relationship is fitted for the filtered rain categories  $R < 2$  mm/hr,  $2$  mm/hr  $\leq R < 10$  mm/hr and  $R \geq 10$  mm/hr. The rain categories  $R \geq 5$  mm/hr & drops  $\geq 1000$ ,  $z \geq 30$  dBZ & drops  $\geq 500$  and  $R \geq 1$  mm/hr are also considered for comparing Singapore fits with the fit of  $\mu$ - $\Lambda$  relations for Florida, Gadanki and Scotland (Dumfries & Galloway-P and Dumfries & Galloway-T). Root mean square deviations show that a linear fit works better at lower rain rates.

The Florida curve lies between the Singapore  $\mu$ - $\Lambda$  relation for the categories  $R < 2$  mm/hr and  $2$  mm/hr  $\leq R < 10$  mm/hr. This indicates that the rain events used by [5] are near our stratiform and transition type rains. The Gadanki curve is closer to the Singapore's  $\mu$ - $\Lambda$  relation for  $R \geq 10$  mm/hr. Both of the DG fits have lowest  $\mu$  values of all the curves. This indicates that their rain events are very weak. The trend of the  $\mu$ - $\Lambda$  fits of Singapore and Florida, for rain rates greater than 5 mm/hr and rain counts greater than 1000 drops, are similar at higher  $\mu$  values of above 4. However, it is found that the fits for Singapore and Gadanki, derived for reflectivities greater than 30 dBZ and rain counts greater than 500 drops, are similar at most of the lower rain rates. The Gadanki curve has higher  $\mu$  values and the Florida curve has lower  $\mu$  values at low rain rates as compared to Singapore's  $\mu$ - $\Lambda$  relationship. The use of JWD at Singapore and Gadanki has more measurement errors and leads to higher  $\mu$  values at these locations. Video distrometer data from Florida and laser distrometers have produced lower  $\mu$  values. The fitting procedure which uses the higher order 6th moment at Gadanki and Florida leads to the higher values of gamma model parameters. Even though Singapore and Gadanki use same measuring instrument, the higher  $\mu$  values of Gadanki curve compared to Singapore curves may be due to the use of 6th moment in their fitting procedure.

The changes in  $\mu$ - $\Lambda$  fits are higher for different climate zones, since each zone has different types of rain events and also depend on the selection of events (either more stratiform or more convective). The use of different distrometers for the measurement of DSD makes a big



difference in the  $\mu$ - $\Lambda$  fits. The  $\mu$ - $\Lambda$  fits of higher rain rates always have less error and at lower rain rates, especially stratiform events, a linear fit is more suitable than polynomial fits. The type of fitting procedure also makes differences in  $\mu$ - $\Lambda$  fits.

Two polarimetric variables found from the T-Matrix calculations and best  $\mu$ - $\Lambda$  fits are used to find the three gamma model parameters. The rain rates are retrieved from the three gamma model parameters. These retrieved rain rates are compared with the measured rain rates for the rain event on the February 26th, 1995. The  $\mu$ - $\Lambda$  fit for the rain category,  $R \geq 5$  mm/hr & drops  $\geq 1000$  can be used for the rain rate retrieval at all the rain rates whereas the retrieval for convective events is more accurate if the  $\mu$ - $\Lambda$  fit for the rain category  $R \geq 10$  mm/hr is used.

## ACKNOWLEDGMENT

The authors would like to thank Prof. Merhala Thurai (Colorado State University, USA) for providing the *T*-Marix code used in this paper. The authors are grateful to anonymous reviewers for their constructive comments and suggestions for the paper.

## REFERENCES

1. Mandeep, J. S., "Equatorial rainfall measurement on Ku-band satellite communication downlink," *Progress In Electromagnetics Research*, Vol. 76, 195–200, 2007.
2. Zhang, G., J. Vivekanandan, and E. Brandes, "A method for estimating rain rate and drop size distribution from polarimetric Radar measurements," *IEEE Transactions on Geoscience and Remote Sensing*, Vol. 39, No. 4, 830–840, Apr. 2001.
3. Ulbrich, C. W., "Natural variation in the analytical form of the raindrop size distribution," *J. Climate Appl. Meteor.*, Vol. 22, No. 10, 1764–1775, 1983.
4. Gurvich, A. S. and V. Kan, "Structure of air density irregularities in the stratosphere from spacecraft observations of stellar scintillation: 1. Three-dimensional spectrum model and recovery of its parameters," *Atmospheric and Oceanic Physics*, Vol. 39, No. 3, 300–310, 2003.
5. Brandes, E. A., G. Zhang, and J. Vivekanandan, "An evaluation of a drop distribution based polarimetric radar rainfall estimator," *Journal of Applied Meteorology*, Vol. 42, No. 5, 652–660, 2003.

6. Zhang, G., J. Vivekanandan, E. Brandes, R. Menegini, and T. Kozu, "The shape-slope relation in observed gamma raindrop size distributions: Statistical error or useful information?" *Journal of Atmospheric and Oceanic Technology*, Vol. 20, No. 8, 1106–1119, 2003.
7. Seifert, A. K., "On the shape-slope relation of drop size distributions in convective rain," *Journal of Applied Meteorology*, Vol. 44, No. 7, 1146–1151, 2005.
8. Moisseev, D. N. and V. Chandrasekar, "Examination of  $\mu$ - $\Lambda$  relation suggested for drop size distribution parameters," *Journal of Atmospheric and Oceanic Technology*, Vol. 24, No. 5, 847–855, 2007.
9. Anagnostou, M. N., E. N. Anagnostou, J. Vivekanandan, and F. L. Ogden, "Comparison of raindrop size distribution estimates from X-band and S-band polarimetric observations," *IEEE Geosci. Remote Sens. Lett.*, Vol. 4, No. 4, 601–605, Oct. 2007.
10. Cao, Q., G. Zhang, E. Brandes, T. Schuur, A. Ryzhkov, and K. Ikeda, "Analysis of video disdrometer and polarimetric radar data to characterize rain microphysics in Oklahoma," *Journal of Applied Meteorology*, Vol. 47, No. 8, 2238–2255, 2008.
11. Cao, Q. and G. Zhang, "Errors in estimating raindrop size distribution parameters employing disdrometer and simulated raindrop spectra," *Journal of Applied Meteorology and Climatology*, Vol. 48, No. 2, 406–425, 2009.
12. Rao, T. N., N. V. P. Kirankumar, B. Radhakrishna, and D. N. Rao, "On the variability of the shape-slope parameter relations of the gamma raindrop size distribution model," *Geophysical Research Letters*, Vol. 33, L22809, 2006, doi:10.1029/2006GL028440.
13. Brawn, D. and G. Upton, "On the measurement of atmospheric gamma drop-size distributions," *Atmos. Sci. Lett.*, Vol. 9, No. 4, 245–247, 2008.
14. Munchak, S. J. and A. Tokay, "Retrieval of raindrop size distribution from simulated dual-frequency radar measurements," *Journal of Applied Meteorology and Climatology*, Vol. 47, No. 1, 223–239, 2008.
15. Atlas, D. and C. W. Ulbrich, "Drop size spectra and integral remote sensing parameters in the transition from convective to stratiform rain," *Geophysical Research Letters*, Vol. 33, L16803, 2006, doi:10.1029/2006GL026824.
16. Tokay, A., D. A. Short, C. R. Williams, W. L. Ecklund, and K. S. Gage, "Tropical rainfall associated with convective and

- stratiform clouds: intercomparison of disdrometer and profiler measurements,” *Journal of Applied Meteorology*, Vol. 38, No. 3, 302–320, 1999.
17. Caracciolo, C., F. Porcu, and F. Prodi, “Precipitation classification at mid-latitudes in terms of drop size distribution parameters,” *Advances in Geosciences*, Vol. 16, 11–17, 2008.
  18. Gunn, R. and K. D. Kinzer, “The terminal velocity of fall for water droplets in stagnant air,” *J. Metero.*, Vol. 6, No. 4, 243–248, 1949.
  19. Smith, P. L., “Raindrop size distributions: Exponential or gamma — Does the difference matter?” *Journal of Applied Meteorology*, Vol. 42, No. 7, 1031–1034, 2003.
  20. Ulbrich, C. W. and D. Atlas, “Rain microphysics and radar properties: Analysis methods for drop size spectra,” *Journal of Applied Meteorology*, Vol. 37, No. 9, 912–923, 1998.
  21. Tokay, A., A. Kruger, and W. F. Krajewski, “Comparison of drop size distribution measurements by impact and optical disdrometers,” *Journal of Applied Meteorology*, Vol. 40, No. 11, 2083–2097, 2001.
  22. Thurai, M., G. J. Huang, V. N. Bringi, W. L. Randeu, and M. Schonhuber, “Drop shapes, model comparisons, and calculations of polarimetric radar parameters in rain,” *Journal of Atmospheric and Oceanic Technology*, Vol. 24, No. 6, 1019–1032, Jun. 2007.
  23. Beard, K. V. and C. Chuang, “A new model for the equilibrium shape of raindrops,” *J. Atmos. Sci.*, Vol. 44, No. 11, 1509–1524, 1987.